

Dynamics of a Vortex Lattice in an Expanding Polariton Quantum Fluid

Riccardo Panico^{1,2}, Guido Macorini², Lorenzo Dominici², Antonio Gianfrate², Antonio Fieramosca^{2,‡},
Milena De Giorgi², Giuseppe Gigli^{1,2}, Daniele Sanvitto^{2,3,†}, Alessandra S. Lanotte^{2,3,*} and Dario Ballarini²

¹*Dipartimento di Matematica e Fisica E. De Giorgi, Università del Salento, Campus Ecotekne, via Monteroni, Lecce 73100, Italy*

²*CNR NANOTEC, Institute of Nanotechnology, Via Monteroni, 73100 Lecce, Italy*

³*INFN, Sez.Lecce, Via Monteroni, 73100 Lecce, Italy*



(Received 15 June 2020; revised 10 March 2021; accepted 11 June 2021; published 21 July 2021)

If a quantum fluid is driven with enough angular momentum, at equilibrium the ground state of the system is given by a lattice of quantized vortices whose density is prescribed by the quantization of circulation. We report on the first experimental study of the Feynman-Onsager relation in a nonequilibrium polariton fluid, free to expand and rotate. Upon initially imprinting a lattice of vortices in the quantum fluid, we track the vortex core positions on picosecond timescales. We observe an accelerated stretching of the lattice and an outward bending of the linear trajectories of the vortices, due to the repulsive polariton interactions. Access to the full density and phase fields allows us to detect a small deviation from the Feynman-Onsager rule in terms of a transverse velocity component, due to the density gradient of the fluid envelope acting on the vortex lattice.

DOI: 10.1103/PhysRevLett.127.047401

One of the most remarkable characteristics of a Bose-Einstein condensate (BEC) is its response to rotation [1]. Different from a conventional fluid, in the “rotating bucket” experiment a condensate does not rotate with the bucket for angular velocities slower than a critical value [2]. The absence of friction with the bucket walls is a unique property of superfluids, which realize the ideal case of irrotational flow. Yet, the velocity field of superfluids is irrotational up to phase defects, i.e., quantized vortices, which allow the condensate to have a finite angular momentum. As a consequence, for a driving angular frequency larger than a critical value [3], the superfluid breaks into the formation of quantized vortex filaments in 3D, or pointlike vortices in 2D, as observed in superfluid helium and ultracold atomic condensates [4,5]. More generally, quantized vortices are excited states (topological defects) of a quantum fluid which form also without macroscopic rotation of the potential trap, for example, via the Kibble-Zurek mechanism or in turbulent regimes [6,7]. Quantized vortices have also proven to be striking examples of the similarities between the condensed matter, optical, and dilute-gas quantum systems, since complex Ginzburg-Landau equations (CGLEs) describe a vast variety of phenomena such as superconductivity, superfluidity, lasing, and Bose-Einstein condensation [8]. With respect to the optical vortices observed in paraxial vortex beams, CGLEs include light-matter interaction as a Kerr-type nonlinearity [9,10], allowing for the existence of dark vortex solitons in a defocusing nonlinear medium and quantized vortices in a superfluid [11,12].

Exciton-polaritons (polaritons hereafter) are a relatively new example of superfluid [13–15], in which a

macroscopic coherent state is formed even far from the thermal equilibrium condition [16]. Polaritons are bosonic quasiparticles which result from the strong interaction between light and matter in semiconductor microcavities with embedded quantum wells. In most cases, their dynamics is well described by a generalized Gross-Pitaevskii (GP) equation, which takes into account the driven-dissipative character of polaritons [17].

In the past decade, quantized vorticity in polariton fluids was observed under a variety of pumping conditions [18,19]. Highly nonlinear effects on the nucleation of few vortices, and solitons have been shown, as well as their all-optical manipulation and trapping in propagating polariton fluids [20,21]. A major advantage of this system is given by the photonic component, which enables the control over the phase and density profiles of the polariton fluid by optical shaping of the pumping laser beam [22,23]. Additionally, the nonlinear interactions inherited from the excitonic component are orders of magnitude higher than in standard nonlinear media. High-quality samples now available with longer polariton lifetime and reduced density of defects allow us to explore complex configurations of vortices, going beyond previous realizations of a single or few vortices.

In this Letter, we report on the creation demand of a macroscopic lattice of quantized vortices in polariton fluids and the measurement of the evolution of both density and phase. The quantum fluid is free to expand and each vortex has a dual function: It participates to the build up of the rotation, and it acts as a test particle that enables the observation of the dynamics. We measure the lattice rotation and expansion and show that these exhibit a small

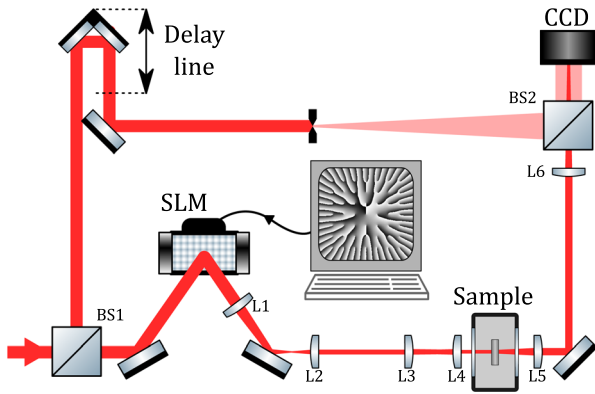


FIG. 1. Schematic representation of the experimental setup. A laser beam is divided in two paths by a beam splitter (BS1) and one beam is diffracted by a SLM, where the phase pattern of a lattice of vortices is displayed. The beam with the imprinted phase profile is imaged on the sample surface by a system of lenses. The signal is made to interfere with a time-delayed reference beam. The interferogram is acquired by a CCD camera, and both density and phase are reconstructed in space and time by digital off-axis holography.

but measurable deviation from the Feynman-Onsager relation. In particular, we observe a detailed balance between the faster radial separation of the vortex cores due to the repulsive polariton-polariton interactions, and a slower rotation of the quantum fluid, yet preserving the regular lattice shape. We model these observations in terms of the initial vortex lattice density, or equivalently, its intervortex spacing, acting as the characteristic scaling length which determines both the expansion rate of the lattice and its instantaneous angular velocity. Finally, we highlight the role of the gradients of quantum fluid density resulting in an additional velocity contribution to the rotation of the lattice, likewise a Magnus effect of classical fluids.

We use a semiconductor planar microcavity with 12 GaAs quantum wells embedded in two distributed Bragg reflectors. A pulsed excitation tuned on resonance with the polariton energy is used to imprint the vortex lattice state [22]. The phase wave front of the exciting beam is modulated by a spatial light modulator (SLM) consisting of an array of individually programmable pixels made of liquid crystal cells. The phase profile of the vortex lattice is designed by software, sent to the SLM, and transferred to the pumping beam upon reflection on the SLM screen. The SLM and the microcavity are conjugate planes in the optical excitation path, with the image of the vortex lattice reduced by a factor 50 in size on the sample surface (see Fig. 1). The exciton-polariton phase profile is inherited from the pulsed laser upon resonant excitation and is free to evolve after the pulse has gone (pulse duration of 2 ps). The time-resolved evolution of the vortex lattice is obtained by interfering the signal coming from the microcavity with a sample of the exciting pulse, as shown in Fig. 1. Digital off-

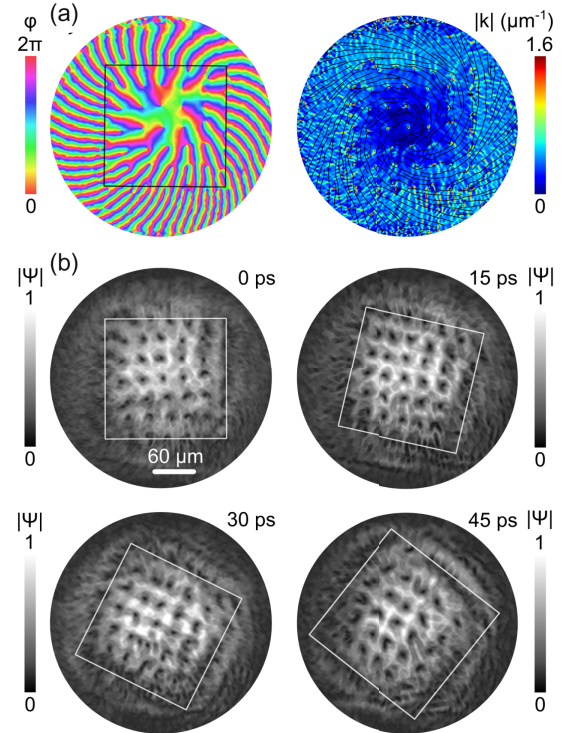


FIG. 2. (a) Phase map $\varphi(\mathbf{r})$ of the initial state of a 7×7 square lattice of vortices (left) with momentum $\mathbf{k}(\mathbf{r}) = \nabla\varphi$ representing the velocity field (right). The color scale of the momentum map is bounded at $|k| = 1.6 \mu\text{m}^{-1}$ to avoid saturation inside the cores. The regular lattice builds up a continuous increase of azimuthal momentum reaching a maximum at its boundary of $\approx 0.42 \mu\text{m}^{-1}$ corresponding to a fluid velocity of $1.2 \mu\text{m ps}^{-1}$. Overlapped streamlines (black lines) display the velocity direction, indicating the rotating motion. (b) The normalized amplitude maps over a span of 45 ps. The outer boundary of the lattice is shown by a square (thin line).

axis holography allows us to retrieve the spatial distribution of both density and phase of the polariton fluid in the 2D plane of the microcavity [24]. By changing the time delay between the pump and the reference, the evolution dynamics of the 2D quantum fluid is obtained in both space and time domain (see Ref. [25] Method section).

The phase and the velocity fields of the initial state of the system with a regular lattice of 7×7 vortices with the same unit topological charge are shown in Fig. 2(a). Because of the internal concentration of vortex charges, the largest momentum is reached at the outer boundary of the region (apart from local fluctuations). The background amplitude profile [Fig. 2(b)] of the lattice is not uniform but modulated by the Gaussian profile of the laser beam. Once the pulsed resonant excitation is over, the polariton lattice rotates in a rigid-body movement, such that the fluid, irrotational for simply connected regions, effectively appears as rotational in a coarse grained picture (in Fig. 2, time shots illustrate the evolution of the polariton density during the first 45 ps).

The velocity circulation around a multiply connected region enclosing a lattice of unitary vortices is quantized according to the Feynman-Onsager relation [30,31], resulting in an angular velocity of the lattice

$$\Omega = \frac{h}{2m} \frac{1}{d^2}, \quad (1)$$

with m the polariton mass and d the intervortex distance [25].

In experiments with superfluid helium [32,33], when the system is put into rotation at constant frequency Ω , at equilibrium a regular lattice of vortices of equal sign unitary charge is formed with an average density in agreement with Eq. (1). Experiments with gaseous BECs in cylindrical traps [34,35] confirm these results with the formation of triangular (or hexagonal) lattices, which are ground state configurations in the rotating frame, containing up to hundreds of vortices. However, in our system, the polariton fluid expands due to the absence of the confining potential, and moreover, a stationary state can never be reached, leading to both the vortex spacing and the rotation frequency to change in time. In order to quantitatively describe the change of the intervortex distance, we can think of the initial condition as that of a rigid-body rotation, in agreement to the Feynman-Onsager relation, with the azimuthal velocity proportional to the distance from the center $v = (\boldsymbol{\Omega} \times \mathbf{r}) \cdot \hat{e}_\theta$. In the absence of interactions, given that the fluid is free to expand, every particle continues to move along a straight line with the initial velocity \mathbf{v} [36]. The intervortex distance $d(t)$ increases following a law of analog form to what is expected for the density of a diffracting optical beam and for an expanding BEC of noninteracting particles after the release from a magnetic trap,

$$d(t) = d_0 \sqrt{1 + \left(\frac{a}{d_0^2} t\right)^2}. \quad (2)$$

Here, d_0 is the initial distance and $a = a_0 \equiv h/2m$ in the linear regime. The expansion factor (a/d_0^2) sets the scaling of all the distances in the lattice. Noteworthy, the circular symmetry of initial velocities is such that any shape, such as the square lattice, appears to be expanding and rotating at later times. This angle of rotation, directly linked to the Gouy phase, can be written upon geometrical considerations as

$$\theta(t) = b \times \arctan\left(\frac{a}{d_0^2} t\right), \quad (3)$$

with the prefactor $b = 1$ in the linear regime, meaning that the limit angle tends to $\pi/2$ for large times. If we add the repulsive interactions between polaritons, the initial mean-field energy is expected to be partially released into kinetic

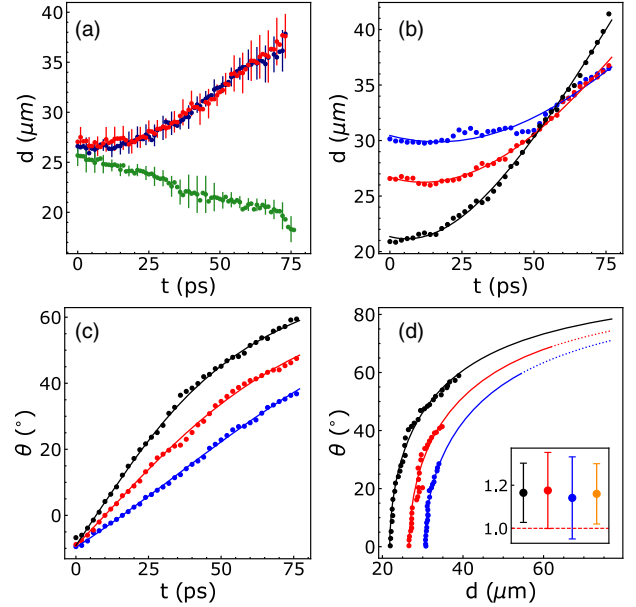


FIG. 3. (a) Intervortex distances over time for three cases with total charge equal to $Q = \pm 49$ (red and blue dots, respectively), and $Q \simeq 0$ (green dots). Error bars come from the estimate of the vortex positions. (b) Mean intervortex distances for three different initial separations and $Q = -49$. (c) The orientation angle of the whole lattice for the same cases as in (b). In panels (b) and (c), solid lines are the best fits of Eqs. (2) and (3), with $a = 11.6 \pm 0.9 \mu\text{m}^2 \text{ps}^{-1}$ and $b = 0.99 \pm 0.09$. The small contraction of the lattice at short time lags, due to a residual curvature of the phase profile of the exciting beam, is taken into account by introducing a time offset t_0 in the fitting functions used in panels (b),(c): $t_0 = 7, 11, \text{ and } 17 \text{ ps}$ for $d_0 = 21, 26.5, \text{ and } 30 \mu\text{m}$, respectively. (d) Rotation angle as a function of the vortex distance during the expansion of the lattice for the three cases shown in panels (b) and (c). Only positive angles are shown in panel (d), i.e., for $t > t_0$, to allow the comparison between different d_0 . Solid lines correspond to the first 150 ps of expansion and rotation. Inset: the value of ab/a_0 as extracted from individual fit [same color legend as in panels (b) and (c)], and for a global fit (yellow point). The deviation from the Feynman-Onsager relation is quantified by the distance from the dashed line, with $a_0 = 9.85 \mu\text{m}^2 \text{ps}^{-1}$ and $b = 1$ of the linear case.

energy during the expansion [37–39]. Nonlinear repulsion marks the origin of a dynamical regime where the vortex trajectories deviate from the straight lines of the linear case due to the earlier onset of an additional radial component of the velocity. As a consequence, in the nonlinear case, the expansion factor in Eqs. (2) and (3) is expected to be always larger than in the linear limit, $a > a_0$.

The evolution of the intervortex distances in regular lattices of same-sign vortices and in a lattice of vortices and antivortices is shown in Fig. 3(a). While the averaged spacing d increases independently of the sign of the circulation ($Q \neq 0$), when the total injected topological charge is null (lattice of vortices and antivortices), the rotation rate is zero [25] and the intervortex spacing slightly

shrinks due to the mutual attraction of vortices with opposite sign. The time behavior of the average spacing d and rotation angle θ measured during the expansion of lattices with different initial intervortex distance d_0 are shown in Figs. 3(b) and 3(c), respectively. The solid lines are the best global fit of Eqs. (2) and (3) to experimental data, showing a very good agreement with a single set of parameters. In Fig. 3(d), the rotation angle is shown as a function of the intervortex separation for the same data reported in Figs. 3(b) and 3(c). These results have been confirmed by independent analysis of numerical simulations (see Ref. [25]).

The rigidlike rotation of the lattice allows us to compare the Feynman-Onsager relation in Eq. (1) with the measurements of the vortex trajectories. Indeed, from Eqs. (2) and (3), we obtain

$$d^2(t) \frac{d\theta(t)}{dt} = ab.$$

Therefore, the angular velocity $d\theta(t)/dt$ is inversely proportional to the squared intervortex distance $d(t)$ during the whole expansion of the lattice, and their product is the same for the three initial d_0 shown in Fig. 3.

In the inset of Fig. 3(d), the product ab is compared to the equilibrium value $a_0 = h/2m$ of Eq. (1), showing a measurable deviation from the Feynman-Onsager relation. The difference is small, but can be appreciated for each separate d_0 , as well as for the global best fit over the three evolutions (yellow point). We ascribe such a deviation to the Magnus effect, i.e., the transversal velocity of the vortex cores induced by density gradients in the polariton fluid [40–42]. In our experiments, the density gradient (similar for the three initial d_0 , since it depends on the Gaussian envelope of the same pumping beam) points radially inward and the Magnus-like velocity accelerates the rotation of the lattice with respect to that of the fluid, $ab > h/2m$.

To highlight the role of nonlinearities in the dynamics, we move to a position on the sample with a higher excitonic fraction (see Ref. [25]). In Fig. 4(a), the trajectories of a vortex pair in the polariton fluid are compared to the straight ones of the linear case. The faster increase of the intervortex distance, with respect to the linear evolution, is shown in Fig. 4(b) for an experimental dataset at $\mu = 0.12$ meV. From Fig. 4(a), it can be seen that a faster expansion implies a smaller rotation angle at long times, as shown in Fig. 4(c) by comparing the linear to the nonlinear case. Although the deviation of the rotation angle from the linear evolution becomes significantly appreciable only at longer times, the global fit of expansion and rotation allows us to extract a reliable value for the prefactor b in Eq. (3). In Fig. 4(d), the results for the parameters (a , b) obtained from the experiments shown in Figs. 3 and 4 and from the numerical simulations of GP dynamics are summarized for different chemical potentials. The blue line corresponds to

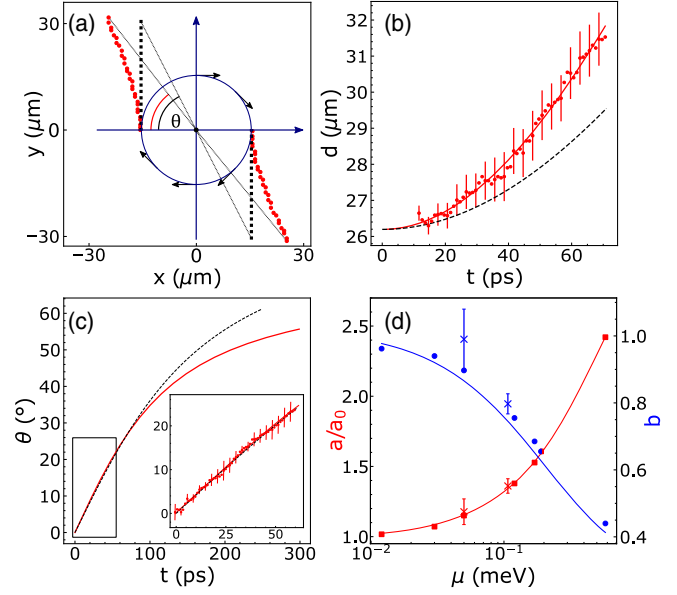


FIG. 4. (a) Graphical representation of the effect of nonlinear interactions producing a bending of the trajectories from the straight lines. (b) The time evolution of the intervortex separation d for a lattice of 5×5 vortices. Red points with error bars are experimental data at chemical potential $\mu = 0.12$ meV (corresponding to a polariton density $n \sim 100 \mu\text{m}^{-2}$, with an interaction strength $g = 10^{-3}$ meV μm^2), and the red solid line is the result of a numerical simulation at equal μ ; from the best fit, the corresponding nonlinear expansion factor is $a = 1.38a_0$. The black dashed line is the evolution in the linear case corresponding to $\mu \approx 0$ meV, and $a = a_0 = 5.04 \mu\text{m}^2 \text{ps}^{-1}$. (c) Rotation angles as a function of time corresponding to the lattice expansions shown in (b). Red line is the best fit of Eq. (3) with $a = 1.38a_0$ and $b = 0.8$; the black dashed line is the angle evolution in the linear case ($a = a_0$, $b = 1$). In the inset, an enlargement at small time lag shows the experimental data (red points) superposed to the best fit (red line). (d) Parameters (a , b) extracted from experiments (crosses) and simulations (circles, squares) at different values of μ . The red line is a polynomial fit to a values; the blue line is the expected behavior for b in the absence of the Magnus effect, a_0/a .

the curve $b = a_0/a$ expected without the Magnus contribution. Both experiments and simulations show a small but measurable deviation from the blue line. If the cores are in the parabolic region of the Gaussian envelope, the added velocity scales up linearly with r , without disturbing the regular lattice shape. However, the effect of additional local density gradients due to the presence of neighboring vortices increases the distortion of the lattice from the regular shape, adding noise to the measurements. Furthermore, the strength of the interactions is responsible for sustaining on a longer time the rigidlike behavior of the lattice dominated by the kinetic energy. In the opposite limit of very small interactions, or waiting enough time in the polariton evolution, this condition may cease to be valid since the intervortex separation becomes comparable to the

healing length, and a new regime may arise, as reported in Ref. [43], and confirmed by our simulations [25].

We have shown that lattices of quantized vortices in out-of-equilibrium, untrapped quantum fluids exhibit a conformal stretching and rotation, compensating the ballistic radial expansion by a decreasing angular velocity. Interactions modify this picture: In our repulsive case, a radial acceleration outward increases the intervortex separation and limits the rotation angle at long times. The vortex lattice behavior is compared to the quantized circulation of the whole fluid, showing a Magnus-like effect as an additional rotation of the vortex lattice with respect to the fluid. These results show the crucial importance of having experimental access to a well-resolved space or time tracking of the vortices in an expanding fluid, where nonlinear effects rapidly weaken. Such a high degree of control over the nonequilibrium dynamics of interacting quantum fluids opens up the possibility to achieve configurations with a larger vortex density and *ad hoc* all-optical confining potentials. It is still an open question whether turbulentlike regimes akin to what is realized in other systems [44,45] will be within reach in exciton-polariton fluids.

We thank Marc E. Brachet, Natalia Berloff, and Ricardo Carretero for useful discussions. The authors acknowledge the Progetto di Rilevante Interesse Nazionale “Interacting Photons in Polariton Circuits INPhoPOL” (Project No. PRIN 2017P9FJBS_001), the project “TECNOMED—Tecnopolo di Nanotecnologia e Fotonica per la Medicina di Precisione” (MUR Decreto Direttoriale n. 3449 del 4/12/2017, CUP B83B17000010001), and the Bilateral Agreement CNR/RFBR (Italy/Russia) 2021–2023,” Hardware implementation of a polariton neural network for neuromorphic computing.

*Corresponding author.

alessandrasabina.lanotte@cnr.it

†daniele.sanvitto@cnr.it

‡Present address: Division of Physics and Applied Physics, School of Physical and Mathematical Sciences, Nanyang Technological University, Singapore.

- [1] A. L. Fetter, Rotating trapped Bose-Einstein condensates, *Rev. Mod. Phys.* **81**, 647 (2009).
- [2] A. J. Leggett, Superfluidity, *Rev. Mod. Phys.* **71**, S318 (1999).
- [3] K. W. Madison, F. Chevy, W. Wohlleben, and J. Dalibard, Vortex Formation in a Stirred Bose-Einstein Condensate, *Phys. Rev. Lett.* **84**, 806 (2000).
- [4] E. L. Andronikashvili and Y. G. Mamaladze, Quantization of macroscopic motions and hydrodynamics of rotating helium II, *Rev. Mod. Phys.* **38**, 567 (1966).
- [5] C. F. Barenghi and N. G. Parker, *A Primer on Quantum Fluids*, SpringerBriefs in Physics (Springer Nature, New York, 2016).
- [6] S. Autti, V. V. Dmitriev, J. T. Makinen, A. A. Soldatov, G. E. Volovik, A. N. Yudin, V. V. Zavjalov, and V. B. Eltsov, Observation of Half-Quantum Vortices in Topological Superfluid ^3He , *Phys. Rev. Lett.* **117**, 255301 (2016).
- [7] *Quantized Vortex Dynamics and Superfluid Turbulence*, edited by C. F. Barenghi, R. J. Donnelly, and W. F. Vinen, Lecture Notes in Physics Book Series (Springer Nature, New York, 2001).
- [8] R. Graham and H. Haken, Laserlight—First example of a second-order phase transition far away from thermal equilibrium, *Z. Phys.* **237**, 31 (1970).
- [9] P. Couillet, L. Gil, and F. Rocca, Optical vortices, *Opt. Commun.* **73**, 403 (1989).
- [10] L. Allen, M. W. Beijersbergen, R. J. C. Spreeuw, and J. P. Woerdman, Orbital angular momentum of light and the transformation of Laguerre-Gaussian laser modes, *Phys. Rev. A* **45**, 8185 (1992).
- [11] A. S. Desyatnikov, Y. S. Kivshar, and L. Torner, in *Progress in Optics*, edited by E. Wolf (Elsevier, New York, 2005), Vol. 47, Chap. 5, pp. 291–391.
- [12] P. G. Kevrekidis, D. J. Frantzeskakis, and R. Carretero-González, *The Defocusing Nonlinear Schrödinger Equation: From Dark Solitons to Vortices and Vortex Rings* (Society for Industrial and Applied Mathematics, Philadelphia, 2015).
- [13] I. Carusotto and C. Ciuti, Probing Microcavity Polariton Superfluidity Through Resonant Rayleigh Scattering, *Phys. Rev. Lett.* **93**, 166401 (2004).
- [14] A. Amo, J. Lefrère, S. Pigeon, C. Adrados, C. Ciuti, I. Carusotto, R. Houdré, E. Giacobino, and A. Bramati, Superfluidity of polaritons in semiconductor microcavities, *Nat. Phys.* **5**, 805 (2009).
- [15] G. Lerario *et al.*, Room-temperature superfluidity in a polariton condensate, *Nat. Phys.* **13**, 837 (2017).
- [16] D. Caputo *et al.*, Topological order and thermal equilibrium in polariton condensates, *Nat. Mater.* **17**, 145 (2018).
- [17] I. Carusotto and C. Ciuti, Quantum fluids of light, *Rev. Mod. Phys.* **85**, 299 (2013).
- [18] K. G. Lagoudakis, Quantized vortices in an exciton-polariton condensate, *Nat. Phys.* **4**, 706 (2008).
- [19] G. Tosi, G. Christmann, N. G. Berloff, P. Tsotsis, T. Gao, Z. Hatzopoulos, P. G. Savvidis, and J. J. Baumberg, Geometrically locked vortex lattices in semiconductor quantum fluids, *Nat. Commun.* **3**, 1243 (2012).
- [20] D. Sanvitto *et al.*, All-optical control of the quantum flow of a polariton condensate, *Nat. Photonics* **5**, 610 (2011).
- [21] T. C. H. Liew, Y. G. Rubo, and A. V. Kavokin, Generation and Dynamics of Vortex Lattices in Coherent Exciton-Polariton Fields, *Phys. Rev. Lett.* **101**, 187401 (2008).
- [22] L. Dominici *et al.*, Interactions and scattering of quantum vortices in a polariton fluid, *Nat. Commun.* **9**, 1467 (2018).
- [23] R. Hivet, E. Cancellieri, T. Boulier, D. Ballarini, D. Sanvitto, F. M. Marchetti, M. H. Szymańska, C. Ciuti, E. Giacobino, and A. Bramati, Interaction-shaped vortex-antivortex lattices in polariton fluids, *Phys. Rev. B* **89**, 134501 (2014).
- [24] S. Donati, L. Dominici, G. Dagvadorj, D. Ballarini, M. De Giorgi, A. Bramati, G. Gigli, Y. G. Rubo, M. H. Szymańska, and D. Sanvitto, Twist of generalized skyrmions and spin

- vortices in a polariton superfluid, *Proc. Natl. Acad. Sci. U.S.A.* **113**, 14926 (2016).
- [25] See Supplemental Material at <http://link.aps.org/supplemental/10.1103/PhysRevLett.127.047401> for methods, different configurations, and numerical simulations. This includes Refs. [26–29].
- [26] C. Ciuti, V. Savona, C. Piermarocchi, A. Quattropani, and P. Schwendimann, Role of the exchange of carriers in elastic exciton-exciton scattering in quantum wells, *Phys. Rev. B* **58**, 7926 (1998).
- [27] A. Minguzzi, S. Succi, F. Toschi, and M. P. Tosi, Numerical methods for atomic quantum gases with applications to Bose-Einstein condensates and to ultracold fermions, *Phys. Rep.* **395**, 223 (2004).
- [28] D. Gottlieb and S. A. Orszag, *Numerical Analysis of Spectral Methods: Theory and Applications* (Society for Industrial and Applied Mathematics, Philadelphia, 1977).
- [29] A. L. Fetter and A. A. Svidzinsky, Vortices in a trapped dilute Bose-Einstein condensate, *J. Phys. Condens. Matter* **13**, R135 (2001).
- [30] R. P. Feynman, in *Progress in Low Temperature Physics* (Elsevier, New York, 1955), Vol. 1, Chap. II, pp. 17–53.
- [31] R. J. Donnelly, Quantized vortices and turbulence in helium II, *Annu. Rev. Fluid Mech.* **25**, 325 (1993).
- [32] E. J. Yarmchuk, M. J. V. Gordon, and R. E. Packard, Observation of Stationary Vortex Arrays in Rotating Superfluid Helium, *Phys. Rev. Lett.* **43**, 214 (1979).
- [33] G. P. Bewley, D. P. Lathrop, and K. R. Sreenivasan, Visualization of quantized vortices, *Nature (London)* **441**, 588 (2006).
- [34] J. R. Abo-Shaeer, C. Raman, J. M. Vogels, and W. Ketterle, Observation of vortex lattices in Bose-Einstein condensates, *Science* **292**, 476 (2001).
- [35] C. Raman, J. R. Abo-Shaeer, J. M. Vogels, K. Xu, and W. Ketterle, Vortex Nucleation in a Stirred Bose-Einstein Condensate, *Phys. Rev. Lett.* **87**, 210402 (2001).
- [36] D. Rozas, C. T. Law, and G. A. Swartzlander, Propagation dynamics of optical vortices, *J. Opt. Soc. Am. B* **14**, 3054 (1997).
- [37] M. O. Mewes, M. R. Andrews, N. J. vanDruten, D. M. Kurn, D. S. Durfee, and W. Ketterle, Bose-Einstein Condensation in a Tightly Confining dc Magnetic Trap, *Phys. Rev. Lett.* **77**, 416 (1996).
- [38] M. J. Holland, D. S. Jin, M. L. Chiofalo, and J. Cooper, Emergence of Interaction Effects in Bose-Einstein Condensation, *Phys. Rev. Lett.* **78**, 3801 (1997).
- [39] C. H. Schunck, M. W. Zwierlein, A. Schirotzek, and W. Ketterle, Superfluid Expansion of a Rotating Fermi Gas, *Phys. Rev. Lett.* **98**, 050404 (2007).
- [40] Y. S. Kivshar, J. Christou, V. Tikhonenko, B. Luther-Davies, and L. M. Pismen, Dynamics of optical vortex solitons, *Opt. Commun.* **152**, 198 (1998).
- [41] R. Navarro, R. Carretero-Gonzalez, P. J. Torres, P. G. Kevrekidis, D. J. Frantzeskakis, M. W. Ray, E. Altuntas, and D. S. Hall, Dynamics of a Few Corotating Vortices in Bose-Einstein Condensates, *Phys. Rev. Lett.* **110**, 225301 (2013).
- [42] T. Simula, Vortex mass in a superfluid, *Phys. Rev. A* **97**, 023609 (2018).
- [43] V. Schweikhard, I. Coddington, P. Engels, V. P. Mogendorff, and E. A. Cornell, Rapidly Rotating Bose-Einstein Condensates in and near the Lowest Landau Level, *Phys. Rev. Lett.* **92**, 040404 (2004).
- [44] J. Salort *et al.*, Turbulent velocity spectra in superfluid flows, *Phys. Fluids* **22**, 125102 (2010).
- [45] N. Navon, A. L. Gaunt, R. P. Smith, and Z. Hadzibabic, Emergence of a turbulent cascade in a quantum gas, *Nature (London)* **539**, 72 (2016).